Inhibition of atherogenesis by the COP9 signalosome subunit 5 in vivo

Yaw Asare[a,b,c], Miriam Ommer[a], Florence. A. Azombo[c], Setareh Alampour-Rajabi[b], Marieke Sternkopf[b], Maryam Sanati[b], Marion J. Gijbels[d,e], Corinna Schmitz[a], Dzmitry Sinitski[a], Pathricia V. Tilstam[b], Hongqi Lue[c], André Gessner[f], Denise Lange[b], Johannes A. Schmid[g], Christian Weber[d,h,i], Martin Dichgans[a,j], Joachim Jankowski[b], Ruggero Pardi[k], Menno P. J. de Winther[e,h], Heidi Noels[b,1,2], and Jürgen Bernhagen[a,c,i,j,1,2]

[a]Institute for Stroke and Dementia Research, Klinikum der Universität München, Ludwig-Maximilians-University, 81377 Munich, Germany; [b]Institute for Molecular Cardiovascular Research, Rheinisch-Westfälische Technische Hochschule Aachen University, 52074 Aachen, Germany; [c]Institute of Biochemistry and Molecular Cell Biology, Rheinisch-Westfälische Technische Hochschule Aachen University, 52074 Aachen, Germany; [d]Cardiovascular Research Institute Maastricht, Maastricht University, 6229 Maastricht, The Netherlands; [e]Department of Medical Biochemistry, Academic Medical Center, University of Amsterdam, 1105AZ Amsterdam, The Netherlands; [f]Institute of Clinical Microbiology and Hygiene, University Hospital of Regensburg, 93053 Regensburg, Germany; [g]Center for Physiology and Pharmacology, Department of Vascular Biology and Thrombosis Research, Medical University Vienna, 1090 Vienna, Austria; [h]Institute for Cardiovascular Prevention, Ludwig-Maximilians-University Munich, 80336 Munich, Germany; [i]Munich Heart Alliance, 80802 Munich, Germany; [j]Munich Cluster for Systems Neurology, 81377 Munich, Germany; and [k]School of Medicine and Scientific Institute, Vita-Salute San Raffaele University, 20123 Milan, Italy

Edited by Michael Karin, University of California, San Diego, School of Medicine, La Jolla, CA, and approved February 21, 2017 (received for review November 13, 2016)

Constitutive photomorphogenesis 9 (COP9) signalosome 5 (CSN5), an isopeptidase that removes neural precursor cell-expressed, developmentally down-regulated 8 (NEDD8) moieties from cullins (thus termed "deNEDDylase") and a subunit of the cullin-RING E3 ligase-regulating COP9 signalosome complex, attenuates proinflammatory NF-κB signaling. We previously showed that CSN5 is up-regulated in human atherosclerotic arteries. Here, we investigated the role of CSN5 in atherogenesis in vivo by using mice with myeloid-specific *Csn5* deletion. Genetic deletion of *Csn5* in *Apoe*$^{-/-}$ mice markedly exacerbated atherosclerotic lesion formation. This was broadly observed in aortic root, arch, and total aorta of male mice, whereas the effect was less pronounced and site-specific in females. Mechanistically, *Csn5* KO potentiated NF-κB signaling and proinflammatory cytokine expression in macrophages, whereas HIF-1α levels were reduced. Inversely, inhibition of NEDDylation by MLN4924 blocked proinflammatory gene expression and NF-κB activation while enhancing HIF-1α levels and the expression of M2 marker *Arginase 1* in inflammatory-elicited macrophages. MLN4924 further attenuated the expression of chemokines and adhesion molecules in endothelial cells and reduced NF-κB activation and monocyte arrest on activated endothelium in vitro. In vivo, MLN4924 reduced LPS-induced inflammation, favored an antiinflammatory macrophage phenotype, and decreased the progression of early atherosclerotic lesions in mice. On the contrary, MLN4924 treatment increased neutrophil and monocyte counts in blood and had no net effect on the progression of more advanced lesions. Our data show that CSN5 is atheroprotective. We conclude that MLN4924 may be useful in preventing early atherogenesis, whereas selectively promoting CSN5-mediated deNEDDylation may be beneficial in all stages of atherosclerosis.

COP9 signalosome | atherosclerosis | inflammation | NEDDylation | MLN4924

Atherosclerosis is the primary cause of cardiovascular diseases. As a chronic inflammatory condition of the vessel wall, atherosclerosis is characterized by endothelial cell activation resulting in the secretion of chemoattractant proteins such as CCL2 and macrophage migration inhibitory factor (MIF) and by increased expression of adhesion molecules such as intercellular adhesion molecule-1 (ICAM-1) and vascular cell adhesion molecule-1 (VCAM-1). These molecules synergize to sequentially recruit inflammatory cells such as monocytes and T lymphocytes into the vessel wall (1–3).

The transcription factor NF-κB plays a crucial role in vascular inflammation and atherogenesis, e.g., by controlling the expression of inflammatory cytokines, chemokines, and adhesion molecules that orchestrate the recruitment and adhesion of leukocytes. Also, numerous genes that regulate differentiation, survival, and proliferation of vascular and immune cells involved in the inflammatory response are targets of NF-κB (4). In resting cells, the NF-κB dimer, p65 and p50, is inactivated by binding to the inhibitor of κB (IκB)-α protein. Inflammatory challenges such as LPS or TNF-α exposure trigger the phosphorylation of IκB-α by the IKK complex (5) and its polyubiquitination by the cullin-RING E3 ubiquitin ligase (CRL) S-phase kinase-associated protein 1 (SKP1)-CUL1/RBX1-βTrCP CRL ($SCF^{\beta TrCP}$), containing cullin-1 (CUL-1) and RING protein ring-box 1 (RBX1) as the enzymatic core, SKP1 as an adaptor, and the β-transducin repeat-containing protein (βTrCP) as substrate-binding F-box protein (6).

Significance

Atherosclerosis is an inflammatory condition of the artery wall and main cause of myocardial infarction and stroke. Inflammatory processes evoking atherogenic lesions involve NF-κB–dependent endothelial-cell activation and monocyte/macrophage recruitment. Constitutive photomorphogenesis 9 (COP9) signalosome (CSN) subunit 5 (CSN5) and the CSN control cullin/RING E3 ligase-dependent degradation of cell-cycle regulators and inhibitor of κB-α by cleaving neural precursor cell-expressed, developmentally down-regulated-8 (NEDD8) from cullins. CSN5 promotes tumorigenesis in humans. We generated a conditional KO mouse in which macrophage/granulocyte-CSN5 is deleted. We show that CSN5 suppresses macrophage inflammation and that mice lacking myeloid CSN5 develop larger atherosclerotic lesions. The NEDDylation inhibitor MLN4924 attenuates early atherosclerosis and inhibits inflammation in macrophages and endothelial cells. With MLN4924 in clinical trials, deNEDDylation approaches may qualify as therapeutics to reduce early-stage atherogenesis.

Author contributions: Y.A., M.P.J.d.W., H.N., and J.B. designed research; Y.A., M.O., F.A.A., S.A.-R., M. Sternkopf, M. Sanati, M.J.G., C.S., D.S., P.V.T., H.L., and D.L. performed research; A.G., J.A.S., C.W., and R.P. contributed new reagents/analytic tools; Y.A., M. Sternkopf, M.J.G., C.S., D.S., H.L., M.P.J.d.W., H.N., and J.B. analyzed data; and Y.A., M.D., J.J., H.N., and J.B. wrote the paper.

The authors declare no conflict of interest.

This article is a PNAS Direct Submission.

Freely available online through the PNAS open access option.

[1]To whom correspondence may be addressed. Email: hnoels@ukaachen.de or juergen.bernhagen@med.uni-muenchen.de.

[2]H.N. and J.B. contributed equally to this work.

This article contains supporting information online at www.pnas.org/lookup/suppl/doi:10.1073/pnas.1618411114/-/DCSupplemental.

Ubiquitinated IκB-α is degraded, releasing the NF-κB dimer to drive gene transcription.

By using KO and transgenic models, differential roles of NF-κB at several stages in the atherogenic process have been demonstrated (7, 8), suggesting that there is a complex and cell type-specific role of the canonical NF-κB pathway in atherosclerosis, which needs further investigation.

Activation of NF-κB depends on a number of control mechanisms, e.g., at the level of its inhibitor IκB-α. CRL-driven IκB-α ubiquitination is controlled by the constitutive photomorphogenesis 9 (COP9) signalosome complex (CSN). The CSN is a highly conserved, multifunctional protein complex of eight subunits (CSN1–CSN8), the 3D structure of which has recently been solved and which has sequence and structural homologies to the 19S lid subcomplex of the 26S proteasome (9, 10). The CSN is involved in various cellular processes such as cell cycle control, DNA repair, and gene expression (11). Catalyzed by the JAMM (JAB1-MPN-domain metalloenzyme) motif of CSN5 [also known as c-Jun activation domain binding protein-1 (JAB1)], a well-described enzymatic activity of the CSN is the cleavage of ubiquitin-like neural precursor cell-expressed developmentally down-regulated 8 (NEDD8) conjugates from the cullin subunit of CRLs, including SCF-type CRLs (12, 13). CSN5 is the only CSN subunit with catalytic activity and acts as part of the holocomplex and independently of the CSN (11). Importantly, CSN5 has also been linked to inflammatory regulation (14–16). Whereas the conjugation of NEDD8 to cullins, termed NEDDylation, is required for an optimal ubiquitin ligase activity of the SCFs (17–20), CSN-mediated deNEDDylation has been linked with the dissociation of the substrate-binding module from the SCF complex and with inhibition of SCF-mediated substrate ubiquitination in vitro (21, 22). A multistep enzymatic process, involving the transfer of matured NEDD8 from a NEDD8-activating E1 onto a NEDD8-conjugating E2 enzyme and finally onto target proteins via an E3 ligase, governs NEDDylation (23).

Inhibition of NEDDylation by the pharmacological agent MLN4924, which blocks E1 activity (24), results in an increase of phosphorylated IκB-α (p-IκB-α) and consequently reduced NF-κB activation in B-cells, myeloid leukemia cells, macrophages, and endothelial cells (25–28). Similarly, signal-induced turnover of IκB-α was shown to be reduced by the deNEDDylating protein CSN5 in endothelial cells (29) and cervical cancer cells (30), reducing NF-κB activation (29). This stabilizing effect of CSN5 toward IκB-α in stimulated cells was explained by the association of the CSN with the deubiquitinase USP15 (30) and by CSN5-mediated deNEDDylation of cullins, controlling SCF activity (11). Overall, MLN4924 and CSN5 both reduce NEDDylation and are involved in the regulation of NF-κB activation.

We recently observed that CSN5 is overexpressed in human atherosclerotic lesions, particularly in the endothelium, as well as in macrophage foam cells, upon atheroprogression (29). We also reported that CSN5 negatively affected inflammatory processes in endothelial cells in vitro (29), prompting us to speculate that CSN5 and deNEDDylation might have an atheroprotective function in vivo. Here, we tested this hypothesis and examined whether myeloid-born CSN5 and the cullin NEDDylation inhibitor MLN4924 were able to reduce atherosclerosis in vivo.

Results

Myeloid-Specific Deletion of *Csn5* Exacerbates Atherosclerosis. To test the hypothesis that CSN5 confers atheroprotection in vivo, *LysM-Cre/Csn5^{floxflox}/Apoe$^{-/-}$* mice, referred to hereafter as *Csn5^{Δmyeloid}/Apoe$^{-/-}$*, with myeloid-specific deletion of the *Csn5* gene (*SI Appendix*, Fig. S1), and control *Csn5^{floxflox}/Apoe$^{-/-}$* littermate mice, referred to hereafter as *Csn5^{wt}/Apoe$^{-/-}$*, were fed a high-fat diet for 12 wk. All mice appeared healthy with no abnormalities. Serum cholesterol, triglyceride levels, leukocyte counts, and weight of mice did not differ between groups (*SI Appendix*, Tables S1 and S2).

Myeloid-specific deletion of *Csn5* in male mice resulted in markedly larger atherosclerotic lesions in the aortic root (Fig. 1*A*), the aorta (Fig. 1*B*), and the aortic arch (Fig. 1*C*) compared with corresponding controls. Analysis of plaque cellular composition in the aortic root revealed comparable content of macrophages, neutrophils, and smooth muscle cells (SMCs); collagen content was also unaltered (*SI Appendix*, Fig. S2 *A–D*).

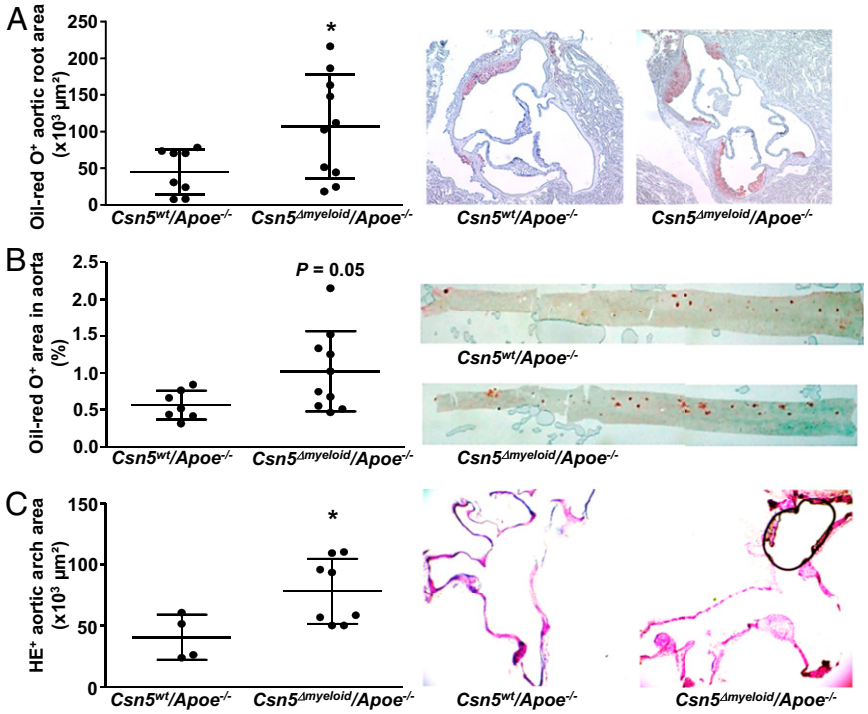

Fig. 1. Myeloid-specific deletion of *Csn5* increases atherosclerosis. Male *Csn5^{wt}/Apoe$^{-/-}$* and *Csn5^{Δmyeloid}/Apoe$^{-/-}$* mice consumed a high-fat diet for 12 wk. Lesion size in aortic root (*A*) and aorta (*B*), as well as aortic arch (*C*), was quantified. Data are means ± SD of $n \geq 8$ mice and representative stainings. Two-tailed *t* test was performed for comparison of *Csn5^{wt}/Apoe$^{-/-}$* vs. *Csn5^{Δmyeloid}/Apoe$^{-/-}$*; $^{*}P < 0.05$).

No differences were observed in apoptosis, although the plaque necrotic core was significantly larger in the absence of *Csn5* in myeloid cells (*SI Appendix*, Fig. S2 *E* and *F*). Also, the number of proliferating macrophages per plaque area was not changed upon myeloid *Csn5* deficiency (*SI Appendix*, Fig. S2*G*). An increase in plaque size was also observed in the aorta, mainly in the abdominal aorta, of female $Csn5^{\Delta myeloid}/Apoe^{-/-}$ mice, although it was less pronounced than in male mice (*SI Appendix*, Fig. S3*A*). Root lesions in female mice were not altered in size (*SI Appendix*, Fig. S3*B*), indicating site-specific effects.

In conclusion, the atherosclerotic phenotype of the *Csn5* gene-deficient mice suggests that Csn5 attenuates atherosclerotic lesion formation in vivo.

Deficiency of *Csn5* Promotes a Proinflammatory Profile in Macrophages. As *Csn5* deficiency increased the size of atherosclerotic lesions without affecting the lesional inflammatory cell content, we examined the effect of *Csn5* deletion on the gene-expression profile of macrophages by using bone marrow-derived macrophages (BMDMs) from $Csn5^{\Delta myeloid}/Apoe^{-/-}$ vs. $Csn5^{wt}/Apoe^{-/-}$ mice. There was an appreciable deletion of *Csn5* (60–70%) on an mRNA and protein level (*SI Appendix*, Fig. S1 *B* and *C*), as reported for other *LysM-Cre*–driven deleted genes (31). *Csn5* deletion also affected levels of the CSN3 and CSN8 subunits of the CSN complex (*SI Appendix*, Fig. S1*D*), indicating inactivation of the entire CSN complex. Surface expression of the macrophage marker F4/80 was not significantly changed upon *Csn5* deficiency (*SI Appendix*, Fig. S1*E*).

Csn5-deficient macrophages and WT controls were stimulated with the inflammatory reagent LPS for 0–24 h. *Csn5* deletion led to a significant increase in *Il-12* and *Il-6* mRNA levels 6 and/or 24 h after LPS stimulation (Fig. 2*A*). Also, after 24 h, LPS-induced secretion of bioactive Il-12p70 was increased upon *Csn5* deletion (Fig. 2*B*, *Left*). Given our recent observation that CSN5 regulates the stability of IκB-α in human endothelial cells (29), and as NF-κB activation is a trigger of inflammatory cytokine production in atherogenesis, we examined whether the effect on gene expression was associated with the NF-κB pathway. We noted a significant decrease in basal IκB-α levels upon *Csn5* deletion. Also, the strong LPS-induced degradation rate of IκB-α was further enhanced by *Csn5* deficiency at early time points (Fig. 2*C*), indicating an increase in NF-κB activation in response to *Csn5* deletion. Similar results were obtained when macrophages were treated with TNF-α, a relevant inflammatory stimulus in atherogenesis, with *Csn5* deficiency enhancing TNF-α–induced Il-12p70 secretion (Fig. 2B, *Right*) and NF-κB activation (Fig. 2*D*). Furthermore, the NF-κB–regulating micro-RNAs (miRs) *miR-146a* and *mi-R21*, both induced in macrophages upon LPS treatment, failed to be up-regulated in $Csn5^{\Delta myeloid}/Apoe^{-/-}$ cells, with miR-21 significantly reduced in $Csn5^{\Delta myeloid}/Apoe^{-/-}$ cells at 6 and 24 h after LPS stimulation compared with control. *Csn5* deficiency did not ablate the induction of *miR-155a* upon LPS stimulation, while up-regulation was only slightly reduced compared with $Csn5^{wt}/Apoe^{-/-}$ controls (Fig. 2*E*). The NF-κB–inhibitory protein A20 was not differentially regulated in WT and *Csn5*-deficient macrophages (*SI Appendix*, Fig. S4). These data suggest that, under inflammatory conditions, CSN5-regulated NF-κB activity is a critical mechanism contributing to the inhibitory effects of CSN5 on proinflammatory cytokine production in macrophages.

To further study the effect of Csn5 on proinflammatory macrophage cytokine profiles, we examined the chemokine-like cytokine MIF, which has been shown to drive atherosclerosis (3) and whose secretion is inhibited by CSN5 in endothelial and tumor cells (29, 32). We observed an increased secretion of MIF in *Csn5*-deleted macrophages (Fig. 2*F*). Moreover, in accord with prior observations that CSN5 stabilizes the transcription factor HIF-1α under normoxic and hypoxic conditions (33), *Csn5* deletion led to significantly decreased nuclear levels of HIF-1α upon LPS treatment (Fig. 2*G*). A significant reduction was observed for the HIF-1α target genes (34) *Edn1* and *Opn1* upon *Csn5*-deletion in LPS-stimulated macrophages, whereas c-*Met*

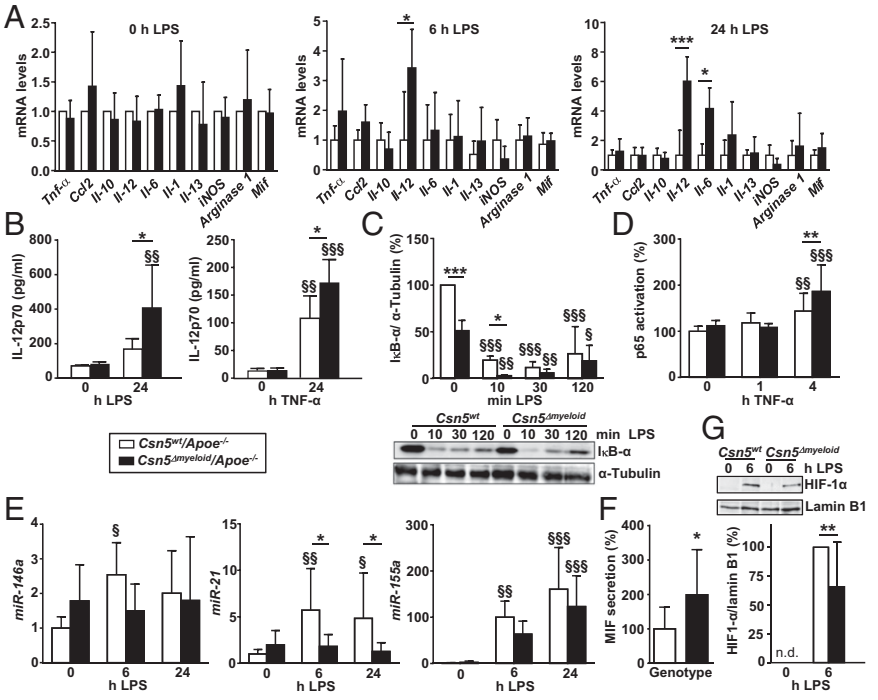

Fig. 2. *Csn5* deficiency promotes a proinflammatory profile in macrophages. BMDMs were isolated from $Csn5^{wt}/Apoe^{-/-}$ and $Csn5^{\Delta myeloid}/Apoe^{-/-}$ mice. (*A*) Cells were stimulated with LPS (100 ng/mL) for 6 and 24 h or left untreated as indicated. Proinflammatory gene expression was determined at baseline (*Left*), after 6 h (*Middle*), and after 24 h (*Right*), and normalized to *Gapdh*. (*B*) Secretion of Il-12p70 was measured in supernatants of cells stimulated with LPS (100 ng/mL, 24 h; *Left*) or TNF-α (20 ng/mL, 24 h; *Right*). (*C*) Immunodetection of IκB-α and α-tubulin in cell lysates of BMDMs treated with LPS for indicated time points: (*Top*) quantification and (*Bottom*) representative blot. (*D*) Cells were stimulated with TNF-α (20 ng/mL; 0–4 h), and p65 activity was quantified relative to untreated control. (*E*) After stimulation with LPS (100 ng/mL), *miR-146a*, *miR-21*, and *miR-155a* were quantified, normalized to *U6*, and expressed relative to unstimulated control. (*F*) Secretion of MIF was measured in supernatants of BMDMs from $Csn5^{wt}/Apoe^{-/-}$ vs. $Csn5^{\Delta myeloid}/Apoe^{-/-}$ mice following culture for 24 h. (*G*) HIF-1α was quantified in nuclear lysates from LPS-stimulated (100 ng/mL, 6 h) cells or untreated control cells. HIF-1α levels were normalized to lamin B1. Representative Western blot is shown. Graphs represent means ± SD of three to six independent experiments, except *E* and *F* ($n \geq 6$). Mann–Whitney test (*F* and *G*) and two-way ANOVA with Bonferroni posttest were performed for comparison between $Csn5^{wt}/Apoe^{-/-}$ and $Csn5^{\Delta myeloid}/Apoe^{-/-}$ (asterisks) and stimulated vs. nonstimulated conditions of same genotype (§; *B–E*; $*/^{\S}P < 0.05$; $**/^{\S\S}P < 0.01$; $***/^{\S\S\S}P < 0.001$).

and *Ets1* were not significantly affected. *Mmp9*, which also is prominently controlled by NF-κB, was up-regulated in *Csn5*-KO inflammatory macrophages (*SI Appendix*, Fig. S5). In line with the lack of effect of *Csn5* deficiency on plaque macrophage proliferation, BMDM proliferation in vitro was not significantly changed upon *Csn5* deficiency (*SI Appendix*, Fig. S6*A*). In conclusion, the deNEDDylating enzyme CSN5 represses inflammatory NF-κB activation and proinflammatory cytokine production in inflammatory macrophages, but also influences the HIF-1α pathway.

Inhibition of NEDDylation by MLN4924 Inhibits Macrophage Inflammatory Responses. Whereas CSN5 induces deNEDDylation by cleaving NEDD8 conjugates from the cullin subunit of CRLs (13), the pharmacological inhibitor MLN4924 inhibits NEDDylation by inhibiting the NEDD8-activating enzyme E1 (NAE) (24). Hence, MLN4924 activity, at least in part, mirrors effects afforded by the overexpression or up-regulation of CSN5, although additional MLN4924 effects may be expected as a result of non-cullin NEDDylation target proteins. Of note, MLN4924 was shown to be generally well tolerated in physiologically active doses in phase I clinical trials in patients with advanced nonhematological malignancies (35) and acute myeloid leukemia and myelodysplastic syndromes (28).

We reasoned that MLN4924-treated macrophages would produce less proinflammatory cytokines in inflammation. BMDMs were isolated from *Apoe*$^{-/-}$ mice and treated with MLN4924 or DMSO control solution. Differentiation of macrophages was not affected by MLN4924, as indicated by similar surface expression of the macrophage marker F4/80 (*SI Appendix*, Fig. S7*A*). Treatment with MLN4924 inhibited cullin-1 NEDDylation (Fig. 3*A* and *SI Appendix*, Fig. S7*B*) and resulted in a significant decrease of LPS-induced proinflammatory gene expression, attenuating the levels of *Tnf-α*, *Il-6*, and *Il-12* after 6 h and those of *Tnf-α*, *Il-6*, *Il-12*, *and Ccl2* after 24 h LPS stimulation (Fig. 3*B*). Also, MLN4924 was able to inhibit basal gene expression of *Tnf-α* and *Il-12* (Fig. 3*B*). On a secreted protein level, LPS-induced production of TNF-α

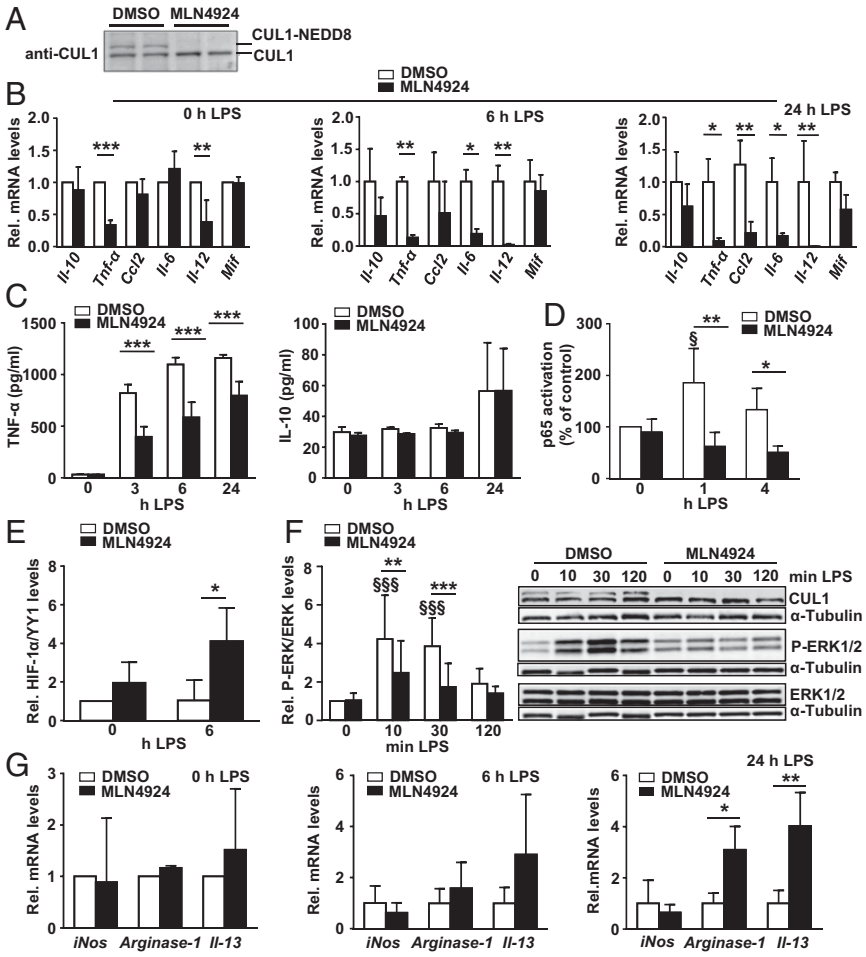

Fig. 3. MLN4924 inhibits proinflammatory cytokine expression and skews macrophage polarization toward M2: involvement of NF-κB, HIF-1α, and ERK signaling. *Apoe*$^{-/-}$ BMDMs were exposed to MLN4924 or DMSO control solution and treated with LPS (100 ng/mL) or left untreated. (*A*) Inhibition of Cullin 1-NEDD8 by MLN4924. (*B*) Proinflammatory gene expression at baseline (*Left*) and 6 h (*Middle*) or 24 h (*Right*) of LPS stimulation, quantified by RT-PCR (normalized to *Gapdh*). (*C*) Effect of MLN4924 or DMSO control on LPS-induced secretion of TNF-α and IL-10 from *Apoe*$^{-/-}$ BMDMs as measured by ELISA. (*D*) Inhibition of LPS (100 ng/mL)-induced p65 DNA binding activity by MLN4924; quantification relative to DMSO control and untreated. (*E*) MLN4924 stabilizes nuclear HIF-1α levels in LPS-treated BMDMs. YY1 was used as nuclear loading control. (*F*) Inhibition of LPS (100 ng/mL)-triggered ERK1/2 MAPK phosphorylation by MLN4924 pretreatment (*Left*, quantification; *Right*, representative Western blot); time course from 0 to 120 min relative to DMSO control and untreated. Total ERK1/2 and tubulin were used as loading control. (*G*) MLN4924 induces gene expression of M2 markers in LPS-stimulated BMDMs. Baseline (*Left*), 6 h LPS (*Middle*), and 24 h LPS (*Right*) normalized to *Gapdh*. (*B*–*G*) Graphs represent means ± SD of $n = 7$ (*F*) or $n = 3$ (*B*–*E* and *G*) independent experiments. Two-way ANOVA with Bonferroni posttest was performed for comparison of DMSO vs. MLN4924-treated cells (asterisks) and stimulated vs. nonstimulated conditions within DMSO- or MLN-treated group (§; */$^{§}P < 0.05$; **/$^{§§}P < 0.01$; ***/$^{§§§}P < 0.001$).

was repressed by MLN4924, whereas IL-10 production was unaffected (Fig. 3*C*). LPS-induced activation of NF-κB was markedly inhibited by MLN4924, although basal NF-κB activation was not affected (Fig. 3*D*). Although this is in line with MLN4924 targeting the NF-κB pathway, we also found that MLN4924 increased nuclear HIF-1α levels in inflammatory-elicited macrophages (Fig. 3*E*), confirming the opposite effect seen in *Csn5*-deficient macrophages, and regulated MAPK signaling. MLN4924 decreased ERK1/2 and (in part) p38 phosphorylation in macrophages stimulated with LPS or TNF-α (Fig. 3*F* and *SI Appendix*, Fig. S8). Macrophage proliferation, similar to what we observed upon *Csn5* deficiency, was not influenced by MLN4924 (*SI Appendix*, Fig. S6*B*).

Together, these data indicate that inhibition of NEDDylation by MLN4924 inhibits the proinflammatory cytokine milieu in macrophages and interferes with NF-κB, HIF-1α, and MAPK signaling in these cells.

MLN4924 Polarizes Macrophages Toward an M2 Phenotype. Atherosclerotic plaques in humans and mice contain M1 and M2 macrophages (36, 37). These subsets of macrophages have been studied extensively in vitro and in various mouse atherosclerosis models, leading to the simplified notion that M1 macrophages, as a result of their inflammatory characteristics, promote plaque inflammation, whereas M2 macrophages resolve it (38). Our observation that MLN4924-treated macrophages expressed lower levels of the classical M1 cytokines (39) *Tnf-α*, *Il-12*, and *Il-6*, prompted us to consider a possible MLN4924-elicited macrophage switch from M1 to M2. To examine this, BMDMs isolated from *Apoe*$^{-/-}$ mice were treated with MLN4924 or DMSO control solvent and challenged with LPS as a surrogate inflammatory stimulus. In addition to the reduced expression of the M1 cytokines observed upon MLN4924 treatment (Fig. 3 *B* and *C*), the antiinflammatory, M2-polarizing cytokine *Il-13* and the M2 marker *Arginase-1* were significantly up-regulated after 24 h of LPS exposure without significantly affecting the M1 marker *iNos* (Fig. 3*G*). This indicates that MLN4924 skews macrophage polarization toward an antiinflammatory M2 state, even in the absence of exogenous, M2 polarizing cytokines such as IL-4.

MLN4924 Inhibits Proatherogenic Gene Expression, Monocyte Arrest, and NF-κB Activation in Inflammatory-Elicited Endothelial Cells. To investigate whether MLN4924 would also affect inflammatory processes in other cell types important in atherosclerosis, we tested its effect on the expression of proatherosclerotic proteins in primary endothelial cells. TNF-α strongly induced the gene expression of the chemokine *CCL2* and the adhesion molecules *VCAM-1* and *ICAM-1* in human umbilical vein endothelial cells (HUVECs), human aortic endothelial cells (HAoECs), and mouse aortic endothelial cells (MAoECs), and MLN4924 treatment essentially completely inhibited these responses, except for CCL2 in MAoECs (Fig. 4*A* and *SI Appendix*, Fig. S9 *A* and *B*). The adhesion molecule *P-selectin* was only moderately up-regulated in MAoECs (*SI Appendix*, Fig. S9*B*), and was not at all up-regulated upon 4 or 8 h of TNF-α stimulation in HUVECs or HAoECs, yet MLN4924 further lowered *P-selectin* expression in both human endothelial cell types after 4 h of TNF-α treatment (Fig. 4*A* and *SI Appendix*, Fig. S9 *A* and *B*), possibly implying an NF-κB–independent mechanism. Adhesion molecules and chemokines act in concert to mediate the arrest of monocytes on activated endothelium of an atherogenic vessel. We performed laminar flow adhesion assays applying resting and TNF-α–activated HUVECs. TNF-α–stimulated HUVECs showed a significant increase in the number of arrested monocytes, and this effect was completely ablated by MLN4924 treatment (Fig. 4*B*).

We next directly tested whether the inhibitory effect of MLN4924 on atherogenic gene expression in primary endothelial cells was at least partly associated with reduced NF-κB signaling. MLN4924 treatment completely inhibited cullin-1 NEDDylation (*SI Appendix*, Fig. S7*C*), and this coincided with the accumulation of phosphorylated IκB-α in HUVECs (Fig. 4*C*) as well as in HAoECs (*SI Appendix*, Fig. S9*C*), indicating that inhibition of cullin-1 NEDDylation impairs the activity of SCF-driven ubiquitination processes. Next, we examined the activation of NF-κB

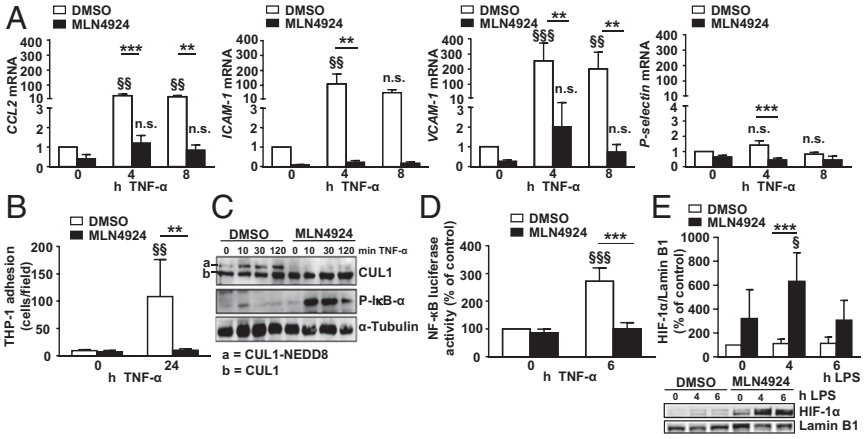

Fig. 4. MLN4924 attenuates proatherosclerotic gene expression, NF-κB activation, and monocyte arrest in inflammatory-elicited endothelial cells while stabilizing HIF-1α. HUVECs were pretreated with MLN4924 or DMSO control solvent and challenged with TNF-α (20 ng/mL) or LPS (100 ng/mL) as indicated. (*A*) Real-time RT-PCR analysis of *CCL2*, *ICAM-1*, *VCAM-1*, or *P-selectin* mRNA levels in TNF-α–stimulated HUVECs. mRNA levels were normalized to *GAPDH* and expressed relative to unstimulated controls. Data represent means ± SD of one representative experiment among four, each performed in triplicate. (*B*) MLN4924 suppresses monocyte adhesion on inflammatory endothelium. Quantification of Calcein-AM–labeled THP1 cells adhered to TNF-α–activated HUVEC monolayers pretreated with MLN4924 or DMSO control. Data represent means ± SD of four independent experiments. (*C* and *D*) MLN4924 attenuates NF-κB activity in endothelial cells. (*C*) Immunodetection of CUL1, p-IκB-α, and α-tubulin in cell lysates from HUVECs treated as indicated. Immunoblots are representative of three independent experiments. (*D*) NF-κB–driven luciferase activity in HUVECs stimulated with TNF-α ($n = 6$) after normalization to β-gal relative to untreated control. (*E*) MLN4924 stabilizes HIF-1α in endothelium. Quantification of HIF-1α levels in nuclear lysates of cells stimulated with LPS vs. untreated. HIF-1α levels were normalized to lamin B1 ($n = 4$). Representative blot is shown. (*A–E*) Data represent means ± SD. Two-way ANOVA with Bonferroni posttest was performed for comparison of MLN4924- vs. DMSO control solution-treated cells (asterisks) and stimulated vs. nonstimulated conditions within DMSO- or MLN-treated group (§; */$^{§}P < 0.05$, **/$^{§§}P < 0.01$, and ***/$^{§§§}P < 0.001$).

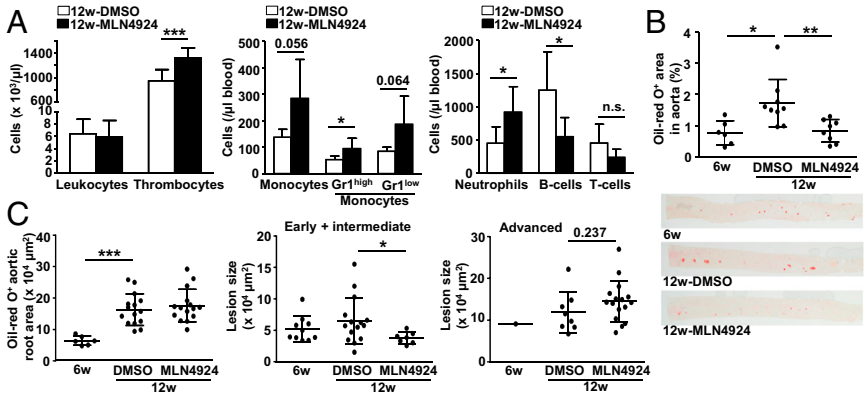

Fig. 5. MLN4924 treatment in vivo reduces the size of early atherosclerotic lesions in aorta and aortic root. Male *Apoe*$^{-/-}$ mice consumed a high-fat diet for 12 wk; in the middle of the diet, mice were treated with 60 mg/kg MLN4924 (12w-MLN4924) or DMSO control solution (12w-DMSO) for 6 wk. Mice that consumed a diet for 6 wk (6w) without any further treatment were used as proof-of-model control. (*A*) Absolute numbers of peripheral blood cells. (*B*) MLN4924 reduces atherosclerotic lesions in aorta. Quantification of lesions in aorta with representative oil red O stainings shown. (*C*) MLN4924 reduces early but not advanced atherosclerotic lesions in aortic root. Quantification of lesions in total aortic root (*Left*) and after classification into early/intermediate (*Middle*) vs. advanced lesions (*Right*). Shown are representative oil red O stainings. (*A*–*C*) Data represent means ± SD of $n \geq 6$ mice. Two-tailed *t* test or Mann–Whitney test was performed as appropriate for comparison between MLN- vs. DMSO-treated groups (*A*); one-way ANOVA with Newman–Keuls or Dunn's posttest was performed as appropriate for comparison of 6 wk and MLN4924- vs. DMSO-treated groups (*B* and *C*; **P* < 0.05, ***P* < 0.01, and ****P* < 0.001; n.s., not significant).

upon MLN4924 preexposure. MLN4924-treated endothelial cells showed a complete inhibition in TNF-α– or LPS-induced NF-κB activation as determined by reporter gene assay (Fig. 4*D* and *SI Appendix*, Fig. S10). As seen in macrophages, MLN4924 also strongly enhanced nuclear HIF-1α levels in LPS-stimulated endothelial cells (Fig. 4*E*).

Together, this indicates that MLN4924 interferes with inflammatory and atherogenic processes in endothelial cells, reflected in reduced atherogenic gene expression, NF-κB activation, and monocyte arrest, and accompanied by HIF-1α stabilization.

Inhibition of NEDDylation by MLN4924 Interferes with Early Atherosclerotic Lesion Formation in Aorta and Root. We next investigated whether MLN4924 would reduce atherosclerosis in vivo, i.e., affecting atherosclerosis pathology opposite to the effect seen upon genetic deletion of the deNEDDylating enzyme Csn5.

To probe the effect of MLN4924 on existent atherosclerotic lesions, male *Apoe*$^{-/-}$ mice were exposed to a high-fat diet. After 6 wk, i.e., when early lesions had developed, thus representing a clinically relevant situation, mice were injected s.c. with 60 mg/kg MLN4924 or with a solvent control solution twice per day on 2 d per week for another 6 wk under continued diet. After a total of 12 wk of high-fat diet, the body weight of the mice, serum cholesterol, triglyceride, and alanine aminotransferase levels, the latter indicating the effect of the inhibitor on the liver, were analyzed and found to be comparable for both groups (*SI Appendix*, Table S3). Analysis of leukocyte subpopulations in blood revealed an increase in thrombocytes and innate immune cells, i.e., neutrophils and monocytes, in the MLN4924-treated group. Among the latter, Gr1^{hi} monocytes were significantly elevated, whereas the increase in the Gr1^{low} subpopulation in the MLN4924-treated group failed to reach statistical significance by a slight margin (Fig. 5*A* and *SI Appendix*, Table S3). At the same time, B-cell numbers were decreased, resulting in overall comparable total leukocyte counts (Fig. 5*A*).

Quantification of lesions showed a significantly reduced lesion area in the descending aorta in the MLN4924-treated group, with MLN4924 treatment reversing atherosclerosis development in the aorta back to baseline levels (Fig. 5*B*). In aortic root, MLN4924 treatment did not influence overall lesion size (Fig. 5*C*). However, lesion classification (*SI Appendix*, Fig. S11*A*) revealed that MLN4924 specifically reduced the size of early- to intermediate-stage lesions but not advanced lesions (Fig. 5*D* and *SI Appendix*, Fig. S11*A*). No significant differences were observed in aortic arch (*SI Appendix*, Fig. S11 *B*-*D*). Plaque characteristics in aortic root were examined next. Although no significant differences were observed in plaque macrophage and smooth muscle cell content, as well as necrotic core area or TUNEL^{+} cell content, between MLN4924- vs. DMSO-treated animals (*SI Appendix*, Fig. S11 *E* and *G*–*I*), collagen content of root lesions was significantly reduced in the MLN4924-treated group (*SI Appendix*, Fig. S11*F*).

In summary, our results indicate that treatment with MLN4924 attenuates the formation of early atherosclerotic lesions in descending aorta and aortic root, whereas more advanced lesions in aortic root or arch were not affected.

MLN4924 Reduces Inflammation in Vivo. We then wished to further study the effect of MLN4924 on the inflammatory response in vivo. We first asked whether our in vitro finding that MLN4924 inhibits atherogenic protein expression in inflammatory endothelial cells and macrophages (Figs. 3 and 4) would be reflected in an in vivo setting. *Apoe*$^{-/-}$ mice fed a high-fat diet for 12 wk were s.c. injected, at halftime of the diet, with 60 mg/kg MLN4924 vs. control solvent twice per day on 2 d per week for 6 wk under continued diet. Serum levels of TNF-α (Fig. 6*A*) were significantly reduced in MLN4924-treated mice, whereas circulating antiinflammatory IL-10 (Fig. 6*A*)

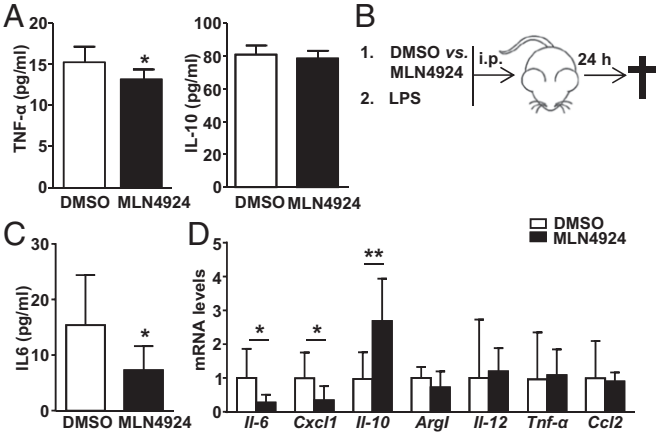

Fig. 6. MLN treatment reduces inflammatory protein expression in vivo. (*A*) Male *Apoe*$^{-/-}$ mice consumed a high-fat diet for 12 wk; in the middle of the diet, mice were injected with MLN4924 or DMSO control solvent for 6 wk. TNF-α and IL-10 levels in serum (n = 8–9). (*B*–*D*) *Apoe*$^{-/-}$ mice pretreated with MLN4924 or DMSO control solution were injected i.p. with LPS (*B*). After 24 h, IL-6 levels were measured in serum (*C*; n = 8–10), and gene expression normalized to *18S* was analyzed in macrophages isolated from the peritoneum (*D*; n = 5–9). (*A*–*D*) Data represent means ± SD. *t* test or Mann–Whitney test was performed: one-tailed (*Il-6* in *D*) or two-tailed (others) as appropriate based on in vitro data (**P* < 0.05 and ***P* < 0.01).

and aortic *Cxcl1* ($P = 0.08$) or aortic adhesion proteins were unaffected (*SI Appendix*, Fig. S12*A*). We finally studied the in vivo effect of MLN4924 on the inflammatory response by interrogating its antiinflammatory capacity in LPS-induced inflammation in mice. MLN4924 pretreatment of mice injected i.p. with LPS strongly reduced serum levels of the inflammatory marker IL-6 (Fig. 6 *B* and *C*), but not TNF-α and CCL2 (*SI Appendix*, Fig. S12*B*). Peritoneal macrophages prepared from LPS-injected mice exhibited significantly decreased expression levels of *Il-6* and *Cxcl1* when isolated from MLN4924-treated vs. control mice, whereas antiinflammatory *Il-10* was increased (Fig. 6*D*). No significant differences were observed for *Tnf-α*, *Ccl2*, *Il-12*, *or Arg-1* (Fig. 6*D*).

In conclusion, these studies demonstrate that MLN4924 not only blocks early atherogenic lesion formation but also various inflammatory mediators known to govern inflammatory processes in vivo.

Discussion

We report on a role of the COP9 signalosome subunit 5 (i.e., CSN5) in attenuating atherogenesis in vivo. We also demonstrate that the pharmacological inhibitor MLN4924, a compound in phase I clinical trials for cancer and known to reduce protein NEDDylation, thereby mimicking CSN5 overexpression, inhibits early atherosclerotic lesion formation in aorta and aortic root as well as acute inflammation in vivo. Both CSN5 and MLN4924 inhibit inflammatory and proatherogenic gene expression through attenuation of NEDD8 conjugation to cullins, and our data suggest that this is, at least partly, the result of a marked negative regulation of the NF-κB pathway (*SI Appendix*, Fig. S13), with additional roles for MAPK signaling and modulation by HIF-1α.

Previous studies described the participation of CSN5 in NF-κB activation in epithelial and T cells (30, 40). We recently extended this to endothelial cells and found CSN5 to attenuate TNF-α–triggered monocyte adhesion on endothelium in vitro. Additionally, we observed an overexpression of CSN5 and two other CSN subunits in atherosclerotic lesions of human carotid arteries upon atheroprogression, a first hint that the CSN may have a functional role in atherogenesis in vivo (29). However, descriptive correlations and in vitro studies frequently cannot predict effects in a complex disease situation in vivo or exclude a bystander role.

Our study clearly reveals enhanced atherosclerotic lesion formation in hyperlipidemic mice lacking *Csn5* in myeloid cells. The antiatherogenic role of CSN5 was more pronounced in male compared with female mice. Whereas *Csn5* deficiency in males led to a broad increase in atherosclerotic lesions in aorta, root, and arch, strong lesion exacerbation in female mice was seen in only the abdominal aorta, with trends in thoracic aorta and aortic arch, whereas no effect was seen in root. Such sex-specific "intensity" effects on atherosclerosis have been reported before. For example, *Cx3cl1* deficiency reduced aortic root lesion size in 12-wk-old female but not male mice, whereas *Pctp* deficiency increased atherosclerosis in male but not female mice (41–45). Various molecular parameters including differences in lipid profiles, cellular responses to oxidized LDL, or NO-dependent endothelial dysfunction have been associated with sex-specific effects in atherosclerosis, but the mechanism has remained unclear in the majority of cases. Atherosclerotic lesions in our study were generally larger in female compared with male $Apoe^{-/-}$ mice, consistent with prior reports (46). The more advanced plaques in females may partly confound atheroprotection by CSN5 in female mice. Also, there may be a CSN5-specific molecular basis for the less pronounced protective effect of CSN5 in females. CSN5/JAB1 was shown to interact with nuclear receptors, preferably progesterone, glucocorticoid, and estrogen receptor, and partially promotes the transactivation activity of these receptors (47).

Exacerbated atherosclerotic lesion formation upon *Csn5* deficiency was not associated with a mere effect on lesional macrophage content, but was linked to inflammatory cytokine production in macrophages. *Csn5*-deficient macrophages exhibited an enhanced expression of inflammatory target genes such as *Il-12* and *Il-6.* The role of IL-6 in atherosclerosis is ambivalent. In early atherosclerosis, IL-6 was found to augment the disease (48), whereas *Il-6*–deficient mice developed more atherosclerosis in advanced stages (49). In conjunction with our MLN4924 in vitro and in vivo data, these findings are in line with the preferential impairment of early vs. advanced atherogenic lesions by CSN5. IL-12 has a more unanimous role in atherosclerosis, with both gene targeting and blockade of IL-12 resulting in reduced atherosclerotic lesions in hyperlipidemic mice (50, 51). Therefore, our observation that *Csn5*-deficient macrophages show an increased production of IL-12 may in part explain exacerbated atherosclerosis development in *Csn5*-KO mice.

As one possible underlying mechanism, *Csn5*-deficient macrophages exhibited a significant decrease in IκB-α levels and an increase in p65 activation, which is in line with reports using epithelial and endothelial cells (29, 30). In support of this notion, *Csn5*-deficiency impaired LPS-induced up-regulation of the NF-κB–regulating miRs *miR-146a* and *miR-21* in macrophages. *MiR-146a* targets TLR4, TRAF6, and IRAK1, thereby antagonizing NF-κB activation (52, 53), and *miR-21* was shown to negatively regulate NF-κB activity through PDCD4 (54). Thus, decreased expression of these miRs contributes to the observed increase in LPS-induced NF-κB activation upon *Csn5* deficiency. In accord, *Csn5* deficiency decreased and MLN4924 stabilized HIF-1α in LPS-elicited macrophages (and endothelial cells). Both *miR-146a* and *-21a* expression levels are coregulated by HIF-1α (55, 56). Decreased *miR-21* and *-146a* levels in *Csn5*-deficient macrophages might thus in part be explained by reduced HIF-1α transcriptional activity. This furthers the conclusion that pathways other than NF-κB contribute to the phenotype seen in *Csn5*-deficient cells. Accordingly, not all genes analyzed in this study were up-regulated even though most are targets of NF-κB. This is in agreement with a prior study in which inhibition of NF-κB did not affect several well-described targets of NF-κB (31). Also, some of the targets, i.e., CCL2, are additionally controlled by other promoter elements such as AP-1. Similarly, pathways influenced by alternative CRL substrates other than IκB-α may contribute to the observed effects in *Csn5*-deficient macrophages.

CSN5 leads to an enhancement of HIF-1α levels in inflammatory macrophages and endothelial cells, in accord with a role for CSN5 and NEDDylation in HIF-1α stabilization (33, 57, 58). Although CSN5 has been suggested to stabilize HIF-1α in a CSN complex-, and thus NEDDylation-, independent manner, MLN4924 was proposed to stabilize HIF-1α, at least in mucosal inflammatory cells, via inhibition of NEDDylation of CUL2, the cullin component present within HIF-1α–ubiquitylating pVHL E3 ligase (59). Given the role for HIF-1α in inflammatory gene expression (60), reduced nuclear HIF-1α may partly explain our finding that not all of the inflammatory genes studied were up-regulated upon *Csn5*-deficiency. Similarly, the observation that not all HIF-responsive genes were decreased upon *Csn5* KO in inflammatory macrophages may be partly explained by counteracting effects of NF-κB activation, e.g., for *c-Met* and *Mmp9*, which are regulated by HIF-1α as well as NF-κB (61).

CSN5 has been reported to regulate the secretion of the inflammatory cytokine MIF (32), which is strongly implicated in atherogenesis (3, 29). Accordingly, *Csn5*-deficient macrophages secreted significant amounts of MIF compared with WT macrophages, despite unaltered *Mif* RNA levels, as expected for this nonclassically secreted mediator. This mechanism may further contribute to increased atherosclerosis in $Csn5^{\Delta myeloid}/Apoe^{-/-}$ mice. Together, CSN5 inhibits atherosclerosis by broadly attenuating the

production of proinflammatory and proatherogenic cytokines in macrophages. These processes involve regulation of NF-κB and HIF-1α signaling.

Recent reports described the NAE blocker MLN4924 as a potent inhibitor of NEDD8 conjugation of cullins (24). We confirmed that MLN4924 treatment of macrophages and endothelial cells predominantly reduced NEDDylation of a cullin protein band. Cullin deNEDDylation reduces ubiquitin ligase activity of CRLs, consequently increasing the stability and transcriptional activity of CRL substrates such as IκB-α or HIF-1α (25, 59). Because of its potential to fine-tune the NF-κB response, and also processes related to cell cycle control or DNA repair by regulating additional CRL targets such as β-catenin, p27, or CDT1, MLN4924 has been successfully used in animal tumor models and is in clinical trials for treatment of leukemia (24, 27, 62). It was shown to be well tolerated in physiologically active doses in phase I clinical trials in patients with advanced nonhematological malignancies (35), acute myeloid leukemia, and myelodysplastic syndromes (28).

Here, we examined the effect of MLN4924 treatment on atherosclerosis in a relevant in vivo mouse model and observed a significant reduction in atherosclerotic lesion size in the aorta and early lesions of aortic root in response to this inhibitor. This was associated with a switch in monocyte-derived macrophages from a pro- to an antiinflammatory phenotype, as indicated by an increase in expression of the M2 macrophage marker *Arginase-1* and the M2-polarizing cytokine *Il-13* in MLN4924-treated macrophages isolated from *Apoe*$^{-/-}$ mice (63). In addition *Tnf-α*, *Il-12*, *Il-6*, *and Ccl2* expression levels were strongly reduced, indicating that macrophages in the MLN4924-treated group produce less inflammatory cytokines. A similar although not identical antiinflammatory phenotype was observed in an in vivo setting when studying macrophages prepared from LPS-injected mice cotreated with MLN4924, with antiinflammatory *Il-10* strongly elevated and proinflammatory cytokines *Il-6* and *Cxcl1* attenuated, whereas markers such as *Tnf-α* and *Il-12* were unchanged. An overall M2/antiinflammatory-polarizing role for MLN4924 is in accord with a recent study revealing that MLN4924 reduces inflammasome-dependent caspase-1 activation in macrophages (64). The inflammasome controls IL-1β secretion, a process typical for M1 (65) but not M2 macrophages (66). Atherosclerotic plaques in humans and mice contain M1 and M2 macrophages (36, 37), and numerous atherosclerosis studies have led to the notion that M1 macrophages promote, whereas M2 macrophages resolve, plaque inflammation (38). Thus, our observation that MLN4924 skews macrophages toward an antiinflammatory/M2 state in vitro and in vivo may at least partially explain the reduced atherosclerotic lesion size in aorta and early root lesions in MLN-treated mice.

MLN4924 inhibited basal gene expression of *Tnf-α* and *Il-12* in macrophages even though basal NF-κB was not affected. This may indicate the involvement of other transcription factors and pathways regulating *Tnf-α* and *Il-12* expression, which may also be regulated by NEDDylation and/or MLN4924. In fact, we found that MLN4924 stabilizes LPS-induced HIF-1α levels, and this effect was in line with observed decreased HIF-1α levels in *Csn5*-deficient cells. Also, MLN4924 reduced MAPK signaling in inflammatory-elicited macrophages. These data are in accord with reports of MLN4924 effects on HIF-1α stabilization in microvascular endothelial cells (26) and MAPK activation in T cells, the latter linked to MLN-induced stabilization of SHC, a negative regulator of ERK signaling that was identified as a target for NEDDylation (67). Interestingly, the pathways identified in our study to be affected by MLN are linked with each other, e.g., reduced NF-κB activity, as observed upon MLN4924, was inversely linked with M2 polarization (68), and *Arginase-1* has been reported to be regulated by HIF-2α (69), which is stabilized by NEDDylation (58).

Our in vitro data add further mechanistic evidence. MLN4924-treated TNF-α–activated endothelial cells express overwhelmingly less *CCL2*, *ICAM-1*, and *VCAM-1*, which may at least partly be explained by reduced NF-κB activation. Interestingly, *P-selectin* was found to be reduced in MLN4924-treated human endothelial cells following 4 h of TNF-α stimulation, although up-regulation by TNF-α per se did not reach significance. This is in line with previous reports showing that human *P-selectin* lacks canonical NF-κB binding sites and is not up-regulated in inflammation (70, 71). A preference for MLN4924 to reduce ICAM-1 and VCAM-1 but not P-selectin levels is consistent with our observation that it markedly reduced monocyte arrest on endothelium. As mentioned, MLN4924 increases LPS-induced HIF-1α levels in endothelial cells, which corresponds with a previous observation of increased HIF activity in the kidney of LPS-treated mice (26). Interestingly, endothelial HIF-1α had been found to promote atherosclerosis and enhance leukocyte adhesion, and myeloid HIF-1α was seen to promote or not affect atherosclerotic lesion formation (60, 72, 73). With respect to our study, this could imply that increased HIF-1α may begin to counteract initial NF-κB–associated atheroprotective effects of MLN4924 implicated in early atherosclerosis and explain the absence of atheroprotection in more advanced lesions. A protective role for MLN4924 in early atherogenesis and endothelial dysfunction is supported by the notion that this compound improves endothelial barrier integrity and disturbed flow/oxidized lipoprotein-elicited NEDDylation-dependent endothelial dysfunction (26, 74).

Importantly, the observed antiinflammatory/antiatherogenic effect of MLN4924 on macrophages and endothelial cells corresponds to its function in vivo. MLN reduced the expression of proinflammatory cytokines in serum of hyperlipidemic and LPS-treated mice. Moreover, MLN reduced the proinflammatory markers *Il-6* and *Cxcl1* in LPS-induced peritoneal macrophages in vivo, whereas *Il-10* was increased. The observation that MLN4924-treated mice only showed a trend toward down-regulation of the arrest chemokine *Cxcl1* or adhesion markers in aortic tissue after 12 wk of high-fat diet might be explained by a counteracting, inducing, effect of endothelial HIF-1α on *Cxcl1* (and other genes), as observed previously in the context of atherosclerosis (73). In fact, our aortic gene expression analysis was performed in late-stage atherosclerosis, when HIF-1α effects may have penetrated to partially override the reduction of NF-κB activation by MLN4924. This notion is supported by our finding that MLN4924 reduced only early atherosclerotic lesions in the aorta and aortic root, but not advanced lesions. Predominant antiatherogenic activity by MLN4924 in early lesions may be the result of disease stage or site specificity, as induced by differences in flow stress at distinct anatomical locations (41). Also, endothelial permeability changes are among the earliest hallmarks of atherosclerosis (2). Thus, barrier function may have already been compromised when MLN treatment was started after 6 wk of Western diet. This might facilitate the influence of circulating Gr1^{high} monocytes or neutrophils, which were elevated upon MLN4924 treatment and may have overcompensated for the early-stage antiinflammatory effects of MLN4924 on endothelium. Such a scenario would be in line with data showing that atherosclerotic lesion size correlates with the number of circulating monocytes (75) and neutrophils (76). Moreover, a selective expansion of myeloid cells paralleled by a decrease in lymphocytes as observed upon MLN treatment of hypercholesterolemic *Apoe*$^{-/-}$ mice was observed before in the context of atherosclerosis and inflammation (77), and may be explained by a competition between granulo- and lymphopoiesis in a common bone marrow niche (78) or by PU1 activity, which is up-regulated by MLN and drives monocyte differentiation (79).

One reason that *Csn5* deficiency does not fully inversely phenocopy effects obtained by MLN4924 treatment might be because the drug was only administered for the last 6 wk of the diet whereas $Csn5^{\Delta myeloid}/Apoe^{-/-}$ mice carried a constitutive deletion of *Csn5* in myeloid cells throughout the entire period. MLN might also have effects independent of CSN-mediated pathways. For example, the target spectrum affected by MLN-induced hypoNEDDylation could be broader than that targeted by selective inhibition of CSN5. Such a notion is supported by the broader spectrum of genes affected by MLN4924 treatment compared with $Csn5^{\Delta myeloid}$ deficiency. It is also conceivable that the spectrum of NEDDylated cullins targeted by MLN4924 and CSN5 differs in relevant atherogenic cell types, affecting different CRL complexes. On the contrary, it is intriguing that MLN4924 treatment (inducing cullin hypoNEDDylation) and CSN inactivation by *Csn5*-gene deficiency (inducing cullin hyperNEDDylation) show the expected opposite effects on NF-κB activity. Previous results indicated in vivo SCF activity to be decreased by CSN overactivation and by complete CSN inactivation, both representing scenarios in which the activity of CRL complexes is compromised (11) (*SI Appendix*, Fig. S13). This may explain why *Csn5*-deficient thymocytes showed reduced steady-state NF-κB activity (40).

With respect to CSN5, the clearness of the identified antiatherogenic (and antiinflammatory) effects is remarkable, as previous studies have also linked CSN5 to proinflammatory JNK/AP1 signaling and proatherogenic LFA-1 integrin activation while counteracting inflammatory MIF activity (14–16). This may be the result of COP9 complex-associated vs. complex-independent activities.

Together, our findings suggest a marked antiatherogenic effect of the deNEDDylation factor CSN5 in myeloid cells in vivo, as well as for the NEDDylation inhibitor MLN4924 in early atherosclerosis, by attenuating inflammatory mechanisms driving atherogenesis. This may argue for novel CSN-related therapies to specifically enhance CSN5 activation, e.g., based on a recently identified molecular trigger implicated in the active/inactive switch of CSN5's isopeptidase activity (80). The observed atheroprotective effect of MLN4924 in early atherosclerosis should stimulate studies to investigate its impact in injury-induced restenosis, in which reendothelialization is a key mechanism to reduce neointimal hyperplasia.

Materials and Methods

Detailed study methods are provided in *SI Appendix*.

Animal Models. C57BL/6 $LysM\text{-}Cre/Csn5^{flox/flox}$ mice were crossed with atherosclerosis-prone C57BL/6 $Apoe^{-/-}$ mice to obtain a myeloid-specific deletion of *Csn5* on $Apoe^{-/-}$ background. To study effects on atherosclerosis, male and female mice were given a high-fat diet for 12 wk, and size and composition of atherosclerotic lesions were assessed by histology and immunofluorescence. To examine the effect of MLN4924 on atherosclerosis, male $Apoe^{-/-}$ mice were fed a high-fat diet for 12 wk. After 6 wk, mice were injected s.c. with 60 mg/kg MLN4924 or control solvent twice per day on two days per week for another 6 wk under continued diet. After a total of 12 wk of diet, mice were killed for analysis of atherosclerosis and gene expression. Furthermore, $Apoe^{-/-}$ mice were injected i.p. with 15 mg/kg MLN4924 vs. control solvent twice per day for a total of 2 d. After 24 h, mice received an i.p. LPS injection (1 μg/mL). After 48 h, mice were killed, and peritoneal macrophages were isolated, adhered for 1 h, and subjected to gene expression analysis.

Cell Culture. HUVECs, HAoECs, MAoECs, and BMDMs were stimulated with 20 ng/mL human or mouse TNF-α or 100 ng/mL LPS as indicated. MLN4924 was dissolved as established (81) and used at a concentration of 500 nmol/L for 2–4 h in all experiments.

Analysis of NF-κB p65 Activity and ELISA. NF-κB p65 DNA binding activity was quantified by using the TransAM NF-κB p65 ELISA (Active Motif) according to the supplier's instructions. NF-κB reporter assays were performed by transfecting an NF-κB luciferase reporter and a β-gal expression construct. After 48 h, cells were exposed to MLN4924 or DMSO control for 16 h, followed by stimulation with TNF-α. Luciferase and β-gal activities were assessed by using Bright-Glo luciferase system and β-gal enzyme assay (Promega).

Cytokine levels of TNF-α, IL-10, IL-12p70, and MIF in serum and/or cell culture supernatant were measured by using commercially available kits.

Macrophage Proliferation and Adhesion Under Laminar Flow. Macrophage proliferation was quantified by using a BrdU-based colorimetric immunoassay (Roche Diagnostics). Adhesion of Calcein-AM–labeled THP1 monocytes on confluent HUVEC monolayers, pretreated with MLN4924 or DMSO control and stimulated with 20 ng/mL human TNF-α as indicated, was quantified in parallel wall chambers under flow (1.5 dyn/cm^2, 4 min) (3).

Quantitative Real-Time PCR and Western Blot Analysis. Quantitative real-time PCR analysis was performed with primers as listed in *SI Appendix*. miRs were isolated by using the miRVana miRNA isolation kit (Thermo Fisher). Quantitative PCR was performed by using the TaqMan MicroRNA Reverse Transcription Kit, TaqMan Gene Expression Master Mix, and predeveloped TaqMan miR assays (*5p* strands; all Thermo Fisher). U6 snRNA was used as reference miRNA.

Total cell lysates were prepared by lysis in RIPA buffer (Pierce) containing protease and phosphatase inhibitors or alternatively in 1× NuPAGE-LDS-sample buffer containing 1 mmol/L DTT. Nuclear extracts were isolated by using a subcellular fractionation kit according to the manufacturer's protocol (Active Motif) or as described previously (82).

Statistical Analysis. Statistical analysis was performed by using GraphPad Prism software (version 5; GraphPad). Data are represented as means ± SD. After testing for normality, data were analyzed by two-tailed Student's *t* test or Mann–Whitney test, one-way ANOVA with Newman–Keuls or Dunn's posttest, or two-way ANOVA with Bonferroni posttest as appropriate. Differences with $P < 0.05$ were considered to be statistically significant.

ACKNOWLEDGMENTS. We thank Dr. E. Shagdarsuren for discussions and Profs. T. Cramer and J. Sluimer for advice on HIF-1α analysis. We thank Roya Soltan, Natalie Ziesch, Michael Lacy, Nadine Persigehl, Melanie Garbe, and Stephanie Elbin for technical assistance. This work was supported by Deutsche Forschungsgemeinschaft (DFG) Graduate School Grant IRTG1508 (to J.B., Y.A., M.P.J.d.W., and C.W.), DFG Grant DFG-SFB1123 (to J.B., M.D., and C.W.), and Interdisciplinary Centre for Clinical Research of RWTH Aachen Medical School Grant IZKF K7/1 (to H.N.); by DFG within the framework of Munich Cluster for Systems Neurology (EXC 1010 SyNergy; J.B. and M.D.), FöFoLe program of Ludwig-Maximilians University Munich (FöFoLe 921; Y.A.), and the Netherlands Organization for Health Research and Development (M.P.J.d.W.); and by CVgenes@target (Health-F2-2013-601456) (M.D.).

1. Hansson GK, Hermansson A (2011) The immune system in atherosclerosis. *Nat Immunol* 12(3):204–212.
2. Weber C, Noels H (2011) Atherosclerosis: Current pathogenesis and therapeutic options. *Nat Med* 17(11):1410–1422.
3. Bernhagen J, et al. (2007) MIF is a noncognate ligand of CXC chemokine receptors in inflammatory and atherogenic cell recruitment. *Nat Med* 13(5):587–596.
4. de Winther MP, Kanters E, Kraal G, Hofker MH (2005) Nuclear factor kappaB signaling in atherogenesis. *Arterioscler Thromb Vasc Biol* 25(5):904–914.
5. Bonizzi G, Karin M (2004) The two NF-kappaB activation pathways and their role in innate and adaptive immunity. *Trends Immunol* 25(6):280–288.
6. Karin M, Ben-Neriah Y (2000) Phosphorylation meets ubiquitination: The control of NF-[κ]B activity. *Annu Rev Immunol* 18:621–663.
7. Gareus R, et al. (2008) Endothelial cell-specific NF-kappaB inhibition protects mice from atherosclerosis. *Cell Metab* 8(5):372–383.
8. Kanters E, et al. (2004) Hematopoietic NF-kappaB1 deficiency results in small atherosclerotic lesions with an inflammatory phenotype. *Blood* 103(3):934–940.
9. Chamovitz DA, et al. (1996) The COP9 complex, a novel multisubunit nuclear regulator involved in light control of a plant developmental switch. *Cell* 86(1):115–121.
10. Lingaraju GM, et al. (2014) Crystal structure of the human COP9 signalosome. *Nature* 512(7513):161–165.
11. Wei N, Serino G, Deng XW (2008) The COP9 signalosome: More than a protease. *Trends Biochem Sci* 33(12):592–600.
12. Lyapina S, et al. (2001) Promotion of NEDD-CUL1 conjugate cleavage by COP9 signalosome. *Science* 292(5520):1382–1385.
13. Cope GA, et al. (2002) Role of predicted metalloprotease motif of Jab1/Csn5 in cleavage of Nedd8 from Cul1. *Science* 298(5593):608–611.

14. Kleemann R, et al. (2000) Intracellular action of the cytokine MIF to modulate AP-1 activity and the cell cycle through Jab1. *Nature* 408(6809):211–216.
15. Bianchi E, et al. (2000) Integrin LFA-1 interacts with the transcriptional co-activator JAB1 to modulate AP-1 activity. *Nature* 404(6778):617–621.
16. Deng Z, et al. (2011) Plant homologue constitutive photomorphogenesis9 (COP9) signalosome subunit CSN5 regulates innate immune responses in macrophages. *Blood* 117(18): 4796–4804.
17. Read MA, et al. (2000) Nedd8 modification of cul-1 activates SCF(beta(TrCP))-dependent ubiquitination of IkappaBalpha. *Mol Cell Biol* 20(7):2326–2333.
18. Wu K, Chen A, Pan ZQ (2000) Conjugation of Nedd8 to CUL1 enhances the ability of the ROC1-CUL1 complex to promote ubiquitin polymerization. *J Biol Chem* 275(41): 32317–32324.
19. Podust VN, et al. (2000) A Nedd8 conjugation pathway is essential for proteolytic targeting of p27Kip1 by ubiquitination. *Proc Natl Acad Sci USA* 97(9): 4579–4584.
20. Kawakami T, et al. (2001) NEDD8 recruits E2-ubiquitin to SCF E3 ligase. *EMBO J* 20(15): 4003–4012.
21. Zhou C, et al. (2001) The fission yeast COP9/signalosome is involved in cullin modification by ubiquitin-related Ned8p. *BMC Biochem* 2:7.
22. Yang X, et al. (2002) The COP9 signalosome inhibits p27(kip1) degradation and impedes G1-S phase progression via deneddylation of SCF Cul1. *Curr Biol* 12(8):667–672.
23. Liakopoulos D, Doenges G, Matuschewski K, Jentsch S (1998) A novel protein modification pathway related to the ubiquitin system. *EMBO J* 17(8):2208–2214.
24. Soucy TA, et al. (2009) An inhibitor of NEDD8-activating enzyme as a new approach to treat cancer. *Nature* 458(7239):732–736.
25. Chang FM, et al. (2012) Inhibition of neddylation represses lipopolysaccharide-induced proinflammatory cytokine production in macrophage cells. *J Biol Chem* 287(42):35756–35767.
26. Ehrentraut SF, et al. (2013) Central role for endothelial human deneddylase-1/SENP8 in fine-tuning the vascular inflammatory response. *J Immunol* 190(1):392–400.
27. Milhollen MA, et al. (2010) MLN4924, a NEDD8-activating enzyme inhibitor, is active in diffuse large B-cell lymphoma models: Rationale for treatment of NF-κB-dependent lymphoma. *Blood* 116(9):1515–1523.
28. Swords RT, et al. (2015) Pevonedistat (MLN4924), a First-in-Class NEDD8-activating enzyme inhibitor, in patients with acute myeloid leukaemia and myelodysplastic syndromes: A phase 1 study. *Br J Haematol* 169(4):534–543.
29. Asare Y, et al. (2013) Endothelial CSN5 impairs NF-κB activation and monocyte adhesion to endothelial cells and is highly expressed in human atherosclerotic lesions. *Thromb Haemost* 110(1):141–152.
30. Schweitzer K, Bozko PM, Dubiel W, Naumann M (2007) CSN controls NF-kappaB by deubiquitinylation of IkappaBalpha. *EMBO J* 26(6):1532–1541.
31. Kanters E, et al. (2003) Inhibition of NF-kappaB activation in macrophages increases atherosclerosis in LDL receptor-deficient mice. *J Clin Invest* 112(8):1176–1185.
32. Lue H, et al. (2007) Macrophage migration inhibitory factor (MIF) promotes cell survival by activation of the Akt pathway and role for CSN5/JAB1 in the control of autocrine MIF activity. *Oncogene* 26(35):5046–5059.
33. Bemis L, et al. (2004) Distinct aerobic and hypoxic mechanisms of HIF-α regulation by CSN5. *Genes Dev* 18(7):739–744.
34. Dengler VL, Galbraith MD, Espinosa JM (2014) Transcriptional regulation by hypoxia inducible factors. *Crit Rev Biochem Mol Biol* 49(1):1–15.
35. Sarantopoulos J, et al. (2016) Phase I study of the investigational NEDD8-activating enzyme inhibitor pevonedistat (TAK-924/MLN4924) in patients with advanced solid tumors. *Clin Cancer Res* 22(4):847–857.
36. Khallou-Laschet J, et al. (2010) Macrophage plasticity in experimental atherosclerosis. *PLoS One* 5(1):e8852.
37. Bouhlel MA, et al. (2007) PPARgamma activation primes human monocytes into alternative M2 macrophages with anti-inflammatory properties. *Cell Metab* 6(2): 137–143.
38. Moore KJ, Sheedy FJ, Fisher EA (2013) Macrophages in atherosclerosis: A dynamic balance. *Nat Rev Immunol* 13(10):709–721.
39. Martinez FO, Helming L, Gordon S (2009) Alternative activation of macrophages: An immunologic functional perspective. *Annu Rev Immunol* 27:451–483.
40. Panattoni M, et al. (2008) Targeted inactivation of the COP9 signalosome impairs multiple stages of T cell development. *J Exp Med* 205(2):465–477.
41. Teupser D, et al. (2004) Major reduction of atherosclerosis in fractalkine (CX3CL1)-deficient mice is at the brachiocephalic artery, not the aortic root. *Proc Natl Acad Sci USA* 101(51):17795–17800.
42. An G, et al. (2009) CD59 but not DAF deficiency accelerates atherosclerosis in female ApoE knockout mice. *Mol Immunol* 46(8-9):1702–1709.
43. Li AC, et al. (2000) Peroxisome proliferator-activated receptor gamma ligands inhibit development of atherosclerosis in LDL receptor-deficient mice. *J Clin Invest* 106(4): 523–531.
44. Matsui Y, et al. (2003) Osteopontin deficiency attenuates atherosclerosis in female apolipoprotein E-deficient mice. *Arterioscler Thromb Vasc Biol* 23(6):1029–1034.
45. Wang WJ, Baez JM, Maurer R, Dansky HM, Cohen DE (2006) Homozygous disruption of Pctp modulates atherosclerosis in apolipoprotein E-deficient mice. *J Lipid Res* 47(11):2400–2407.
46. Meyrelles SS, Peotta VA, Pereira TM, Vasquez EC (2011) Endothelial dysfunction in the apolipoprotein E-deficient mouse: Insights into the influence of diet, gender and aging. *Lipids Health Dis* 10:211.
47. Chauchereau A, Georgiakaki M, Perrin-Wolff M, Milgrom E, Loosfelt H (2000) JAB1 interacts with both the progesterone receptor and SRC-1. *J Biol Chem* 275(12): 8540–8548.
48. Welteke V, et al. (2009) COP9 signalosome controls the Carma1-Bcl10-Malt1 complex upon T-cell stimulation. *EMBO Rep* 10(6):642–648.
49. Schieffer B, et al. (2004) Impact of interleukin-6 on plaque development and morphology in experimental atherosclerosis. *Circulation* 110(22):3493–3500.
50. Davenport P, Tipping PG (2003) The role of interleukin-4 and interleukin-12 in the progression of atherosclerosis in apolipoprotein E-deficient mice. *Am J Pathol* 163(3): 1117–1125.
51. Hauer AD, et al. (2005) Blockade of interleukin-12 function by protein vaccination attenuates atherosclerosis. *Circulation* 112(7):1054–1062.
52. Nahid MA, Satoh M, Chan EK (2011) MicroRNA in TLR signaling and endotoxin tolerance. *Cell Mol Immunol* 8(5):388–403.
53. Ma X, Becker Buscaglia LE, Barker JR, Li Y (2011) MicroRNAs in NF-kappaB signaling. *J Mol Cell Biol* 3(3):159–166.
54. Sheedy FJ, et al. (2010) Negative regulation of TLR4 via targeting of the proinflammatory tumor suppressor PDCD4 by the microRNA miR-21. *Nat Immunol* 11(2): 141–147.
55. Spinello I, et al. (2015) Differential hypoxic regulation of the microRNA-146a/CXCR4 pathway in normal and leukemic monocytic cells: Impact on response to chemotherapy. *Haematologica* 100(9):1160–1171.
56. Liu Y, et al. (2014) A feedback regulatory loop between HIF-1α and miR-21 in response to hypoxia in cardiomyocytes. *FEBS Lett* 588(17):3137–3146.
57. Bae MK, et al. (2002) Jab1 interacts directly with HIF-1alpha and regulates its stability. *J Biol Chem* 277(1):9–12.
58. Ryu JH, et al. (2011) Hypoxia-inducible factor α subunit stabilization by NEDD8 conjugation is reactive oxygen species-dependent. *J Biol Chem* 286(9):6963–6970.
59. Curtis VF, et al. (2015) Stabilization of HIF through inhibition of Cullin-2 neddylation is protective in mucosal inflammatory responses. *FASEB J* 29(1):208–215.
60. Aarup A, et al. (2016) Hypoxia-inducible factor-1α expression in macrophages promotes development of atherosclerosis. *Arterioscler Thromb Vasc Biol* 36(9):1782–1790.
61. Rhee JW, et al. (2007) NF-kappaB-dependent regulation of matrix metalloproteinase-9 gene expression by lipopolysaccharide in a macrophage cell line RAW 264.7. *J Biochem Mol Biol* 40(1):88–94.
62. Soucy TA, Smith PG, Rolfe M (2009) Targeting NEDD8-activated cullin-RING ligases for the treatment of cancer. *Clin Cancer Res* 15(12):3912–3916.
63. Müller U, et al. (2007) IL-13 induces disease-promoting type 2 cytokines, alternatively activated macrophages and allergic inflammation during pulmonary infection of mice with Cryptococcus neoformans. *J Immunol* 179(8):5367–5377.
64. Segovia JA, et al. (2015) Nedd8 regulates inflammasome-dependent caspase-1 activation. *Mol Cell Biol* 35(3):582–597.
65. Dinarello CA (1996) Biologic basis for interleukin-1 in disease. *Blood* 87(6):2095–2147.
66. Martinez FO, Gordon S, Locati M, Mantovani A (2006) Transcriptional profiling of the human monocyte-to-macrophage differentiation and polarization: New molecules and patterns of gene expression. *J Immunol* 177(10):7303–7311.
67. Jin HS, Liao L, Park Y, Liu YC (2013) Neddylation pathway regulates T-cell function by targeting an adaptor protein Shc and a protein kinase Erk signaling. *Proc Natl Acad Sci USA* 110(2):624–629.
68. Wang N, Liang H, Zen K (2014) Molecular mechanisms that influence the macrophage m1-m2 polarization balance. *Front Immunol* 5:614.
69. Takeda N, et al. (2010) Differential activation and antagonistic function of HIF-alpha isoforms in macrophages are essential for NO homeostasis. *Genes Dev* 24(5):491–501.
70. Liu Z, et al. (2010) Differential regulation of human and murine P-selectin expression and function in vivo. *J Exp Med* 207(13):2975–2987.
71. Yao L, et al. (1999) Divergent inducible expression of P-selectin and E-selectin in mice and primates. *Blood* 94(11):3820–3828.
72. Chaudhari SM, et al. (2015) Deficiency of HIF1α in antigen-presenting cells aggravates atherosclerosis and type 1 T-helper cell responses in mice. *Arterioscler Thromb Vasc Biol* 35(11):2316–2325.
73. Akhtar S, et al. (2015) Endothelial hypoxia-inducible factor-1α promotes atherosclerosis and monocyte recruitment by upregulating microRNA-19a. *Hypertension* 66(6): 1220–1226.
74. Pandey D, et al. (2015) NEDDylation promotes endothelial dysfunction: A role for HDAC2. *J Mol Cell Cardiol* 81:18–22.
75. Combadière C, et al. (2008) Combined inhibition of CCL2, CX3CR1, and CCR5 abrogates Ly6C(hi) and Ly6C(lo) monocytosis and almost abolishes atherosclerosis in hypercholesterolemic mice. *Circulation* 117(13):1649–1657.
76. Drechsler M, Megens RT, van Zandvoort M, Weber C, Soehnlein O (2010) Hyperlipidemia-triggered neutrophilia promotes early atherosclerosis. *Circulation* 122(18):1837–1845.
77. Zernecke A, et al. (2008) Protective role of CXC receptor 4/CXC ligand 12 unveils the importance of neutrophils in atherosclerosis. *Circ Res* 102(2):209–217.
78. Ueda Y, Kondo M, Kelsoe G (2005) Inflammation and the reciprocal production of granulocytes and lymphocytes in bone marrow. *J Exp Med* 201(11):1771–1780.
79. Khalife J, et al. (2015) Pharmacological targeting of miR-155 via the NEDD8-activating enzyme inhibitor MLN4924 (Pevonedistat) in FLT3-ITD acute myeloid leukemia. *Leukemia* 29(10):1981–1992.
80. Echalier A, et al. (2013) Insights into the regulation of the human COP9 signalosome catalytic subunit, CSN5/Jab1. *Proc Natl Acad Sci USA* 110(4):1273–1278.
81. Jumpertz S, et al. (2014) The β-catenin E3 ubiquitin ligase SIAH-1 is regulated by CSN5/JAB1 in CRC cells. *Cell Signal* 26(9):2051–2059.
82. Tilstam PV, et al. (2014) Bone marrow-specific knock-in of a non-activatableIkkα kinase mutant influences haematopoiesis but not atherosclerosis in Apoe-deficient mice. *PLoS One* 9(2):e87452.